

DELFT UNIVERSITY OF TECHNOLOGY

REPORT 00-07

THE INFLUENCE OF RELATIVE PERMEABILITY FUNCTIONS ON THE
OIL AND WATER PRODUCTION

F. J. VERMOLEN, G. J. M. PIETERS AND J. BRUINING

ISSN 1389-6520

Reports of the Department of Applied Mathematical Analysis

Delft 2000

Copyright © 2000 by Department of Applied Mathematical Analysis, Delft, The Netherlands.

No part of the Journal may be reproduced, stored in a retrieval system, or transmitted, in any form or by any means, electronic, mechanical, photocopying, recording, or otherwise, without the prior written permission from Department of Applied Mathematical Analysis, Delft University of Technology, The Netherlands.

The influence of relative permeability functions on the oil and water production

F. J. Vermolen, G. J. M. Pieters*, J. Bruining †

March 10, 2000

Abstract

In this paper we analyse the influence of relative permeability functions on the production of oil and water from an oil reservoir. The analysis presented is of practical significance for injection well treatments with polymer gels. First we formulate a test-case with relative permeabilities depending linearly on saturation for which a semi-explicit solution is found. The results from this test-case agree perfectly well with results obtained from a numerical method based on a Finite Volume approach with a higher order discretisation. This numerical method is used for more general shapes of the relative permeability functions of oil and water. First we analyse the Corey-shape relative permeability and subsequently we use more general forms. It is concluded that the shape of the relative permeability function plays an important role in the production of water and oil.

Keywords: hyperbolic equations, Corey-permeabilities, power-law, optimization

1 Introduction

Many mature oil fields (reservoirs) suffer from excessive water production. Large water production creates serious environmental problems concerning water waste disposal. As operating cost increase in the field, it leaves large oil reserves unproduced. A major cause for high water production is water channelling through high permeability layers in reservoirs. This channelled water will cause early breakthrough in the production well and can constitute the major fraction of the produced fluids.

To minimise water production, or to postpone water breakthrough, polymers / gels are injected, aiming at decreasing the permeability of well-permeable layers. The polymers / gels used are hydrophilic, i.e. they easily dissolve in water. Consequently, the water mobility is reduced. Furthermore, the polymers / gels are adsorbed at the skeleton of the porous medium. This causes a decrease of the permeability. Since water flows in the smallest pores of the porous medium, mainly the relative permeability of water is effected. Polymer gel treatments in both the production well and injection well are used. Here our focus is on injection well treatment (see for instance [1], [4]).

In this study we are interested in the influence of the relative permeability functions on the production

*Faculty for Technical Mathematics and Informatics, Delft University of Technology, Mekelweg 4, NL 2628 CD Delft, The Netherlands,

†Faculty of Applied Earth Sciences, Delft University of Technology, P.O. Box 5031, NL 2600 RX Delft, The Netherlands,

of water and oil. For the permeability of oil and water, k_1, k_2 (m^2) we use the concept of relative permeability, given by:

$$\begin{aligned} k_1 &= k_0 k_{r1}, & (\text{water}), \\ k_2 &= k_0 k_{r2}, & (\text{oil}), \end{aligned}$$

where k_0 (m^2) denotes the permeability of the porous medium (reservoir), k_{r1} (-) and k_{r2} (-) respectively denote the relative permeabilities of water and oil. The indices $i = 1$ and $i = 2$ respectively correspond to water and oil. Generally k_{ri} ($i \in \{1, 2\}$) are functions of the saturation S_i (-), which is defined as the volume fraction of void occupied by fluid i (oil or water). As relative permeability functions we first use the classical Corey model and subsequently we treat power-like relative permeability functions. We investigate the relation between the relative permeabilities of oil and water and the production of oil and water by a parametric study.

In this study we consider a single layer with a constant pressure condition (hence an extension to multiple layers can be done easily). First we formulate a mathematical model and specify the relative permeability functions in Section 2. Subsequently we give some analytical aspects on the behaviour of the solution of the equations in Section 3. Furthermore, in Section 3 we give an analytical test-case. The derivation is given Appendix 1. Section 4 gives a description of the results. We end with some conclusions in Section 5.

The nature of this study differs from conventional studies in which technically known relative permeability behaviours are used. Here we use fictitious relative permeability functions to determine the optimal behaviour for the production of water and oil. From the practical point of view it indicates which modification of relative permeability with polymer gels would be optimal.

2 Physical Model

In this section we formulate the mathematical model. First we give the transport equations in terms of a hyperbolic conservation law. Subsequently, we give the pressure equation and finally we state the formulas for the calculation of water and oil production.

2.1 Transport equations

We consider an axially symmetric reservoir of constant thickness, H (m), which extends to R (m). At the central axis a production well with radius r_w (m) ($r_w \ll R$) is present which extends over the full thickness of the reservoir. The reservoir has constant porosity and permeability. We consider two phase flow in porous media. We consider a radial geometry where flow occurs from a cylindrical boundary at $r = R$ towards a production well with a radius $r_w \ll R$ in the center of the reservoir. We assume that the injected polymer gel has uniformly affected the cylindrical reservoir leading to a single relative permeability function in the entire domain. The fluids, oil and water, are immiscible and incompressible. We use the Darcy law of multiphase flow. We disregard capillary pressure in the flow direction. We also assume that in the axial direction capillary forces dominate over gravity forces and hence that the saturation is constant over the height of the reservoir. The saturations do not depend on the axial co-ordinate and only depend on the distance r from the well center.

We assume that the polymer-gels effect the relative permeability. The mass balance equation and the

Darcy law on $r_w < r < R, t > 0$ can be stated:

$$\phi \frac{\partial S_i}{\partial t} + \frac{1}{r} \frac{\partial(rq_i)}{\partial r} = 0, \quad i \in \{1, 2\}, \quad (2.1)$$

$$q_i = -\frac{k_0 k_{ri}}{\mu_i} \frac{\partial p}{\partial r}, \quad i \in \{1, 2\}. \quad (2.2)$$

Here ϕ (-), k_0 (m²), μ_i (Pa s), S_i (-) and q_i (m/s) respectively denote the porosity, permeability of the porous medium, the viscosity, saturation and the volumetric flux (Darcy velocity) of phase i . The pressure is denoted by p (Pa). Equations (1) represent the mass balance equations for incompressible media and equations (2) represent the Darcy law for each phase. Water and oil are respectively denoted by $i = 1$ and $i = 2$. Further, k_{ri} denotes the relative permeability of phase i , note that $k_{r2}(S_2) = k_{r2}(1 - S_1) =: \bar{k}_{r2}(S_1)$. For convenience we omit the overline. Since the pressure is maximal for $r = R$, we have $\partial p / \partial r > 0$ and hence the Darcy velocity is negative. We denote the pressure drop by $\Delta p := p(R) - p(r_w)$ and assume that this pressure drop is given.

We assume the pores to be fully saturated, i.e. $S_1 + S_2 = 1$. Hence from equations (1) follows

$$\frac{1}{r} \frac{\partial}{\partial r} (r(q_1 + q_2)) = 0 \quad \text{for} \quad r_w < r < R, t > 0.$$

Integration of above equation with respect to r gives

$$r \cdot (q_1 + q_2) = q(t) \quad \text{for} \quad r_w < r < R, t > 0. \quad (2.3)$$

Here $q(t)$ is a function of time and we will determine its value and see later that it can be interpreted as a velocity. Equations (2) imply

$$q_2 = \frac{\mu_1 k_{r2}}{\mu_2 k_{r1}} \cdot q_1. \quad (2.4)$$

Combination of equations (3) and (4) yields

$$q_1 = \frac{q(t)}{\left(1 + \frac{\mu_1 k_{r2}(S_1)}{\mu_2 k_{r1}(S_1)}\right) r}. \quad (2.5)$$

We define the fractional flow-function as

$$f(S_1) = \frac{1}{1 + \frac{\mu_1 k_{r2}(S_1)}{\mu_2 k_{r1}(S_2)}}, \quad (2.6)$$

then $q_1 = \frac{q(t)}{r} f(S_1)$. Substitution of above definition into equations (1) gives

$$\phi \frac{\partial S_1}{\partial t} + \frac{q(t)}{r} \frac{\partial f(S_1)}{\partial r} = 0, \quad \text{for} \quad r_w < r < R, t > 0. \quad (2.7)$$

Note that the velocity $q(t)$ is negative since the flow is towards the production in the center of the reservoir. In technical applications there exists a residual oil saturation S_{2r} and a connate water saturation S_{1c} below which there is no flow of oil and water, i.e. respectively for $S_2 < S_{2r}$ (no oil flow) and for $S_1 < S_{1c}$ (no water flow). The initial and boundary conditions (IB) hence become:

$$(IB) \begin{cases} S_1(r, 0) = S_{1c}, & r_w < r < R, \\ S_1(r = R, t) = 1 - S_{2r}, & t > 0. \end{cases}$$

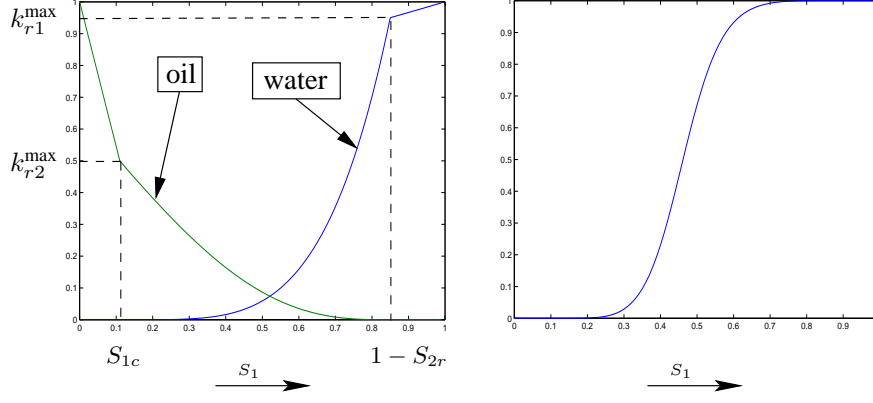


Figure 1: Left the relative permeability functions of oil and water using the model of Corey and right the convex-concave flux function $f(S_1)$. Input data are given the text. Here S_{1c} and S_{2r} respectively represent the connate water and residual oil saturation. The end-point permeabilities are denoted by k_{r1}^{\max} and k_{r2}^{\max} .

2.2 Relative permeability functions

Here we introduce the relative permeability functions that we use in the analysis. First we give the classical Corey functions and subsequently we give the power-law functions. The latter class of functions allows more general shapes.

2.2.1 Corey relative permeability functions

Here we introduce the relative permeability functions according to the Corey model [2]. These functions have been determined empirically. The relative permeability functions depend on the saturation of fluid 1 (water) and the 'sorting factor' β . The 'sorting factor' is an experimental parameter and is not generally defined. It is generally used as a measure for the pore size geometry distribution. A low sorting factor represents a disperse pore size and geometry distribution. These functions are given as follows for $S_{1c} \leq S_1 \leq 1 - S_{2r}$:

$$k_{r1}(S_1) = k_{r1}^{\max} \bar{S}^{-\frac{2+3\beta}{\beta}}, \quad S_1 \in [S_{1c}, 1 - S_{2r}], \quad (2.8)$$

and

$$k_{r2}(S_1) = k_{r2}^{\max} (1 - \bar{S})^2 \left(1 - \bar{S}^{-\frac{2+\beta}{\beta}}\right), \quad S_1 \in [S_{1c}, 1 - S_{2r}], \quad (2.9)$$

Here we defined

$$\bar{S} = \frac{S_1 - S_{1c}}{1 - S_{1c} - S_{2r}}. \quad (2.10)$$

We plotted the relative permeability functions (left) and the flux function (right) obtained from the relative permeability functions in Figure 1. We used the data-set of de Rooij [3]:

$$\begin{aligned} \beta &= 1.5, \\ S_{1c} &= 0.11, & S_{2r} &= 0.15, \\ k_{r1}^{\max} &= 0.50, & k_{r2}^{\max} &= 0.95, \\ \mu_1 &= 1.01 \cdot 10^{-3} \text{Pa s}, & \mu_2 &= 3 \cdot 10^{-3} \text{Pa s}. \end{aligned}$$

Here S_{1c} and S_{2r} respectively represent the connate water and residual oil saturation. Furthermore, k_{r1}^{\max} and k_{r2}^{\max} denote the maximum relative permeability of respectively water and oil.

During this study we limit ourselves to the interval $S_1 \in [S_{1c}, 1 - S_{2r}]$.

2.2.2 Power-like relative permeability functions

Here we give the power-like relative permeability functions in addition to the Corey functions. These functions are given as follows:

$$k_{r1}(\bar{S}) = k_{r1}^{\max} \bar{S}^{\alpha_1}, \quad \text{for } S_1 \in [S_{1c}, 1 - S_{2r}], \quad (2.11)$$

$$k_{r2}(\bar{S}) = k_{r2}^{\max} (1 - \bar{S})^{\alpha_2}, \quad \text{for } S_1 \in [S_{1c}, 1 - S_{2r}]. \quad (2.12)$$

Here \bar{S} has been defined in equation (2.10), α_1 and α_2 are exponents which determine the shape of the relative permeabilities.

2.3 Determination of the production rate

From $q_1 = \frac{q(t)}{r} f(S_1)$ follows for the production of water $P_1(t)$ (m³/s):

$$\begin{aligned} P_1(t) &= -2\pi r_w H \cdot q_1 \Big|_{r=r_w} = -2\pi r_w H \cdot \frac{q(t) f(u(r_w))}{r_w} = \\ &= -2\pi \cdot H q(t) \cdot f(u(r_w)), \end{aligned} \quad (2.13)$$

and for the production of oil $P_2(t)$ (m³/s) we obtain:

$$\begin{aligned} P_2(t) &= -2\pi r_w H \cdot q_2 \Big|_{r=r_w} = -2\pi r_w H \cdot \frac{q(t)}{r_w} (1 - f(u(r_w))) = \\ &= -2\pi H \cdot q(t) \cdot (1 - f(u(r_w))). \end{aligned} \quad (2.14)$$

We use above expressions to compute the production rate of water and oil.

3 Analytical Aspects

In this section we summarise some analytical aspects of the equations. First we introduce a co-ordinate transformation to simplify the equations to obtain a solution. Subsequently we make some qualitative remarks about the behaviour of the solution and we give a test-case for which a semi-explicit solution is obtained.

3.1 Co-ordinate transformation

Consider equation (2.6), then set

$$-\frac{1}{r} \frac{\partial}{\partial r} =: \frac{\partial}{\partial x} \iff \frac{\partial x}{\partial r} = -r, \quad (3.1)$$

this implies $x = -\frac{1}{2}r^2 + k$, where k is a constant of integration. We require the outer boundary of the reservoir (inflow) to co-incide with $x = 0$, $x(r = R) = 0$, hence $x = \frac{1}{2}(R^2 - r^2)$ and

$r = \sqrt{R^2 - 2x}$, ($r > 0$). Using this transformation and defining $Q(t) = -q(t)$ changes equation (2.7) into

$$\frac{\partial S_1}{\partial t} + Q(t) \frac{\partial f(S_1)}{\partial x} = 0. \quad (3.2)$$

Above equation is subject to analysis in the next subsection. We consider above equation for $x \in (0, \frac{1}{2}(R^2 - r_w^2))$ and $t > 0$. Since $\frac{\partial p}{\partial r} > 0$ it follows that $Q(t) > 0$.

3.2 Determination of the shock speed

Using the method of characteristics it can be shown that the solution of equation (3.2) gives the following profiles for the saturation S_1 as a function of position x :

- Shock-waves when the flux-function $f(S_1)$ is convex (i.e. $f''(S_1) \geq 0$),
- Rarefactions when the flux-function $f(S_1)$ is concave (i.e. $f''(S_1) < 0$), profiles are continuous then and satisfy $f'(S_1) = \eta$ with $\eta := \frac{x}{\int_0^t Q(s) ds}$,
- Rarefactions followed by shock-waves when the flux-function is convex-concave (standard Buckley–Leverett).

This can be found in textbooks on hyperbolic equations such as Smoller [7] and Rhee [6]. Subsequently we use the Darcy law to determine the injection rate using a constant pressure condition.

3.2.1 Determination of the injection rate

For the determination of the speed of the shock we use the Darcy law, see equations (2), for radial symmetry hence follows that:

$$\frac{Q(t)}{r} = q_1 + q_2 = k_0 \left(\frac{k_{r1}}{\mu_1} + \frac{k_{r2}}{\mu_2} \right) \frac{\partial p}{\partial r}. \quad (3.3)$$

Above equation is arranged into

$$\frac{\partial p}{\partial r} = \frac{Q(t)}{r} \frac{1}{k_0 \left(\frac{k_{r1}}{\mu_1} + \frac{k_{r2}}{\mu_2} \right)}. \quad (3.4)$$

Direct integration with respect to r gives an expression for the pressure-drop, Δp (Pa), which can be arranged into the following expression for $Q(t)$:

$$Q(t) = k_0 \Delta p \left[\int_{\tilde{\Omega}} \left(\frac{k_{r1}}{\mu_1} + \frac{k_{r2}}{\mu_2} \right)^{-1} \frac{1}{r} dr \right]^{-1}, \quad (3.5)$$

where $\Delta p := p(R) - p(r_w) > 0$ and we define $\tilde{\Omega} := \{r \in \mathbb{R} : r_w < r < R\}$ for convenience. From the co-ordinate transformation (15) follows $\frac{1}{r} dr = -\frac{dx}{R^2 - 2x}$, hence above equation can be written as

$$Q(t) = k_0 \Delta p \left[\int_{\Omega} \left(\frac{k_{r1}}{\mu_1} + \frac{k_{r2}}{\mu_2} \right)^{-1} \frac{dx}{R^2 - 2x} \right]^{-1}. \quad (3.6)$$

Here we defined for convenience $\Omega := \{x \in \mathbb{R} : 0 < x < \frac{1}{2}(R^2 - r_w^2)\}$. Above equation is used to compute the injection rate, $Q(t)$, as a function of time for radial symmetry. Since the profile of S_1 depends on time and the relative permeabilities depend on S_1 , $Q(t)$ is an implicit function of time. Since no explicit relation for the saturation profile is available for the Corey permeability functions, generally we evaluate above integral numerically, except for the test-case described below where we evaluate the integral analytically.

3.2.2 Analytical Testcase

We consider a relatively simple testcase in which the relative permeability are linear, i.e. $n = m = 1$. In addition, we set

$$S_{1c} = S_{2r} = 0, \quad k_{r1} = S_1, \quad \text{and} \quad k_{r2} = 1 - S_1.$$

Of course the extension of above relative permeability functions to $k_{r1} = k_{r1}^{\max} S_1$ and $k_{r2} = k_{r2}^{\max} (1 - S_1)$ is trivial but is omitted here for the sake of illustration. For this case the fluxfunction $f(S_1)$ is concave and the saturation profile exhibits a rarefaction behaviour. In Appendix I we show that the saturation profile satisfies for $0 < t < \tau_1$:

$$S_1(x, t) = \begin{cases} 1, & 0 < x \leq E \xi(t), \\ \frac{1}{1-E} \left\{ \sqrt{\frac{E \xi(t)}{x}} - E \right\}, & E \xi(t) < x < \frac{\xi(t)}{E}, \\ 0, & \frac{\xi(t)}{E} \leq x < L, \end{cases}$$

where $\xi(t) := \frac{1}{\phi} \int_0^t Q(s) ds$, $E := \frac{\mu_1}{\mu_2}$ and τ_1 is the time defined such that $\frac{\xi(t)}{E} = L$. Above saturation profile is substituted into equation (3.6) to give the following ordinary differential equation (ODE) for $\xi(t)$:

$$\phi \xi'(t) = -\frac{k_0 \Delta p}{I(\xi(t))}, \quad t > 0, \quad (3.7)$$

this is done in Appendix I, where the function $I(\xi(t))$ is specified. Above ODE is separable and can be solved either numerically or analytically. The analytical solution requires a lot of tedious algebra. This analytical solution then gives an equation for $\xi(t)$ (see Appendix I for more details), which can be solved directly at each time using a zero-point method instead of a time-integration of a differential equation.

The solution of above equation is substituted into the expression for $S_1(x = L, t)$ to give the saturation at the production well (i.e. $r = r_w$ or $x = L := \frac{1}{2}(R^2 - r_w^2)$). Subsequently we use equations (2.13) and (2.14) to determine the production of water and oil. An example for the production curves of water and oil in barrels per day is given in Figure 2. From Figure 2 it can be seen that at early stages the oil production increases slightly whereas the water production remains zero. Subsequently water starts being produced (increase of water production) and the oil production starts to decrease. This respective increase and decrease looks rather linear.

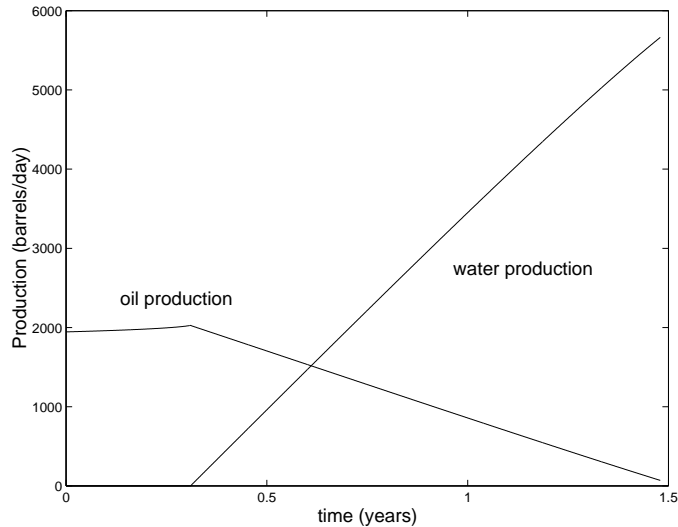


Figure 2: Production curves for oil and water with linear permeabilities using the explicit solution.

4 Numerical Method and Results

First we describe briefly the numerical scheme that has been used to obtain the results in this section. Subsequently we give the calculated results in terms of variation of the sorting factor, end-point permeabilities and connate water saturation. A low sorting factor indicates a disperse pore size distribution.

4.1 Numerical Method

To compute the solution of the transformed equation (3.2), we use a Finite Volume Scheme with an upwind discretisation for the spatial discretisation. Furthermore, we use a higher order (flux-limiter) method for an accurate discretisation of the convective term. As limiter function we use the function of van Leer [8]. For the explicit time discretisation we use a predictor-corrector scheme, which gives a second order accuracy for the time-discretisation (i.e. a Runge–Kutta-2 method).

In this study we are only interested in the qualitative behaviour of the production rate of water and oil as a function of the relative permeability functions and as stated in the physical model description we disregard gravity. From this we hope to find guidelines for an optimal permeability behaviour.

The used numerical scheme has been described in detail by Pieters [5]. Before we describe the results, we compare the numerical results to the results obtained from the testcase. We use the same set as for Figure 2. Figure 3 shows the oil and water production for the same set of parameters as Figure 2 where the explicit solution has been used. The curves in Figure 3 correspond to different numbers of gridnodes. From comparison of the two figures follows that for more than 100 gridnodes the agreement is excellent. For smaller number of gridnodes the profiles become smoother due to numerical diffusion.

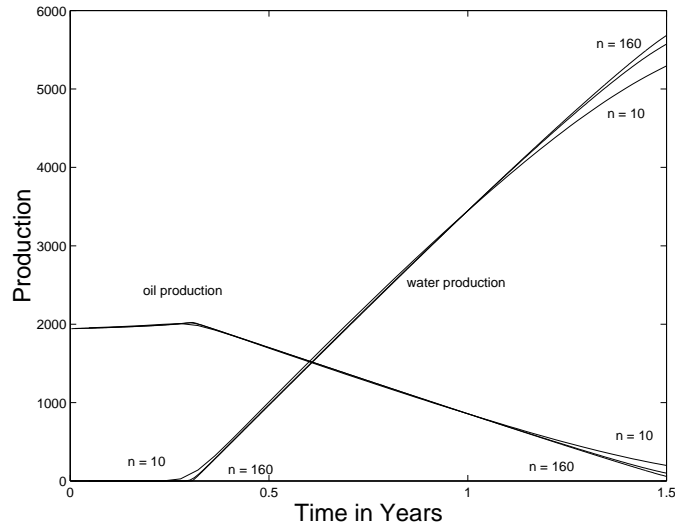


Figure 3: Production curves for oil and water with linear permeabilities using the numerical method for different number of gridnodes. Note the good agreement of the numerical results with those from the explicit solution in Figure 2.

4.2 Results

Except for the relative permeability functions we use the data-set from Table 1. First we consider the Corey-permeabilities and subsequently we treat the power-law permeabilities.

4.2.1 Corey-permeabilities

We use the data-set from Table 1. In the following subsections we change only one parameter per calculation set.

Variation of the sorting factor β

Figure 4 displays production curves for oil and water for different sorting factors. It can be seen that water breakthrough takes place at earlier stages for high sorting factors. Hence a low sorting factor is advantageous. From the Corey-functions follows that the water relative permeability function becomes more curved for high sorting factors. The shape of the relative permeability function for oil does not change significantly. Furthermore the increase of the water production after water breakthrough increases more rapidly for high sorting factors.

Physically the sorting factor appearing in the Corey permeabilities is interpreted as a measure for the pore shape and size distribution: Low sorting factors correspond to disperse pore size distributions. From Figure 4 it appears that a disperse pore size distribution is advantageous. In practice, however, the positive effect of the low sorting factor disappears as gravity segregation occurs.

Variation of the end-point relative permeability of water (k_{r1}^{\max})

Figure 5 displays production curves of oil and water for different maximum relative permeabilities of water. The reduction of the end-point permeability of water is considered as the main target of the use of polymer-gels. It can be seen that water-breakthrough takes place at early stages for high

Parameter	Value	Unit
β	1.5	[-]
S_{1c}	0.11	[-]
k_{r1}^{\max}	0.5	[-]
R	150	[m]
R_w	0.1	[m]
μ_1	$1.01 \cdot 10^{-3}$	[Pa s]
μ_2	$3 \cdot 10^{-3}$	[Pa s]
S_{2r}	0.15	[-]
k_{r2}^{\max}	0.95	[-]
k_0	$2.5 \cdot 10^{-12}$	[m ²]
ϕ	0.30	[-]
Δp	-10^6	[Pa]
H	5	[m]

Table 1

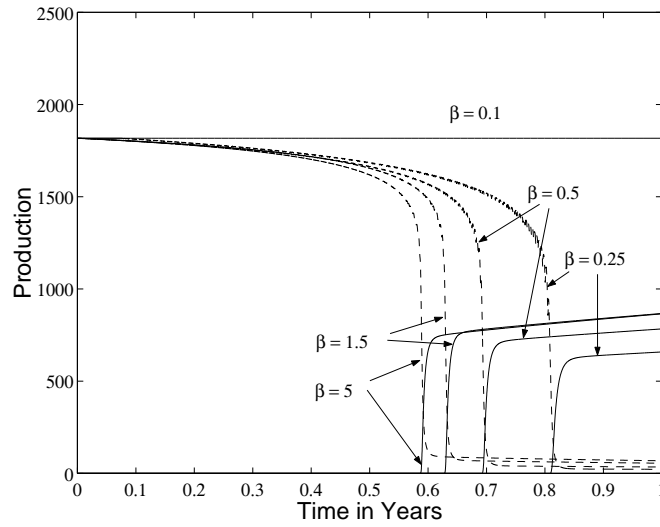


Figure 4: Production curves in barrels per day of oil and water for different values of the sorting factor. All further data are taken from Table 1. The dashed and solid curves respectively correspond to oil and water production.

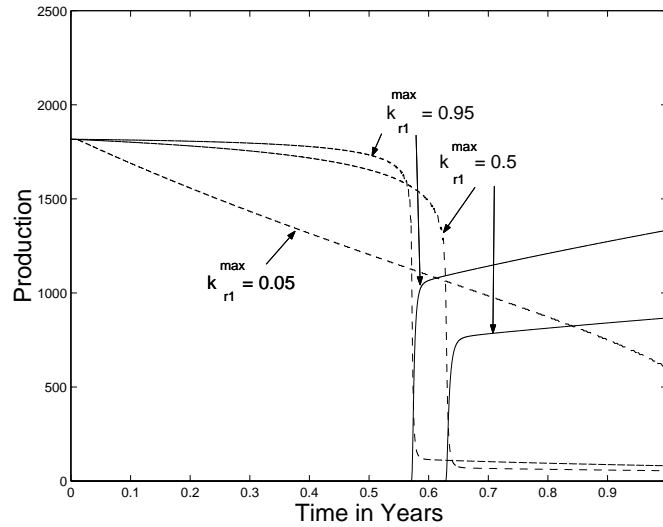


Figure 5: Production curves in barrels per day for different maximum water relative permeability. All further data are taken from Table 1. The dashed and solid curves respectively correspond to oil and water production.

maximum water permeability. However, also the oil production remains at a higher level at the early stages for these high maximum water permeabilities. Furthermore, the water production increase is more pronounced for high maximum water relative permeability. In other words for low end-point water relative permeability the life-time of the reservoir increases whereas the production of oil decreases. The breakthrough of water is delayed. From this point of view the oil is produced faster if the maximum water relative permeability is high but then the subsequent water production (after breakthrough) is also high. This effect leads to a deteriorated production in multi-layered systems.

Variation of the viscosities of water and oil

Figure 6 represents the oil and water production for different values of the water and oil viscosity. We observe that the case of a water viscosity of 1 mPa s and oil viscosity of 30 mPa s gives a low production of oil and a late breakthrough of water. Furthermore, a high water viscosity (30 mPa s) and an oil viscosity of 3 mPa s gives an oil production that is lower than for the case in which the water viscosity of 1 mPa s is used. The shape is similar to the case in which the end-point water permeability is low (see Figure 7). Increasing the water viscosity hence gives lower oil production rates but later water breakthrough. The starting rate of the oil production is not influenced by the water viscosity. An increase of the oil viscosity also delays the breakthrough of water but decreases the oil production rate, this is observed at the start of production.

Variation of the end-point relative permeability of oil k_{r2}^{\max}

Figure 7 displays the oil and water production for different maximum oil relative permeabilities. It can be seen that the production rate is large at the early stages for high maximum oil relative permeabilities. However, the oil production decreases soon for high maximum oil relative permeabilities and water breakthrough takes place soon.

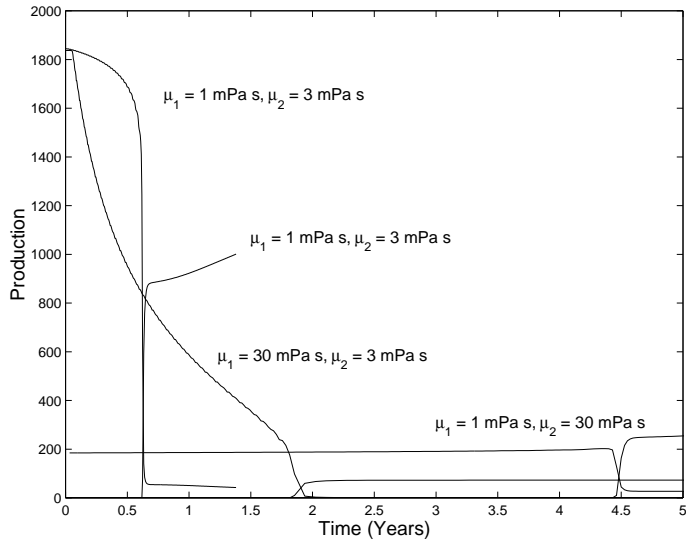


Figure 6: Production curves in barrels per day for different values of the water and oil viscosity. All further data are taken from Table 1.

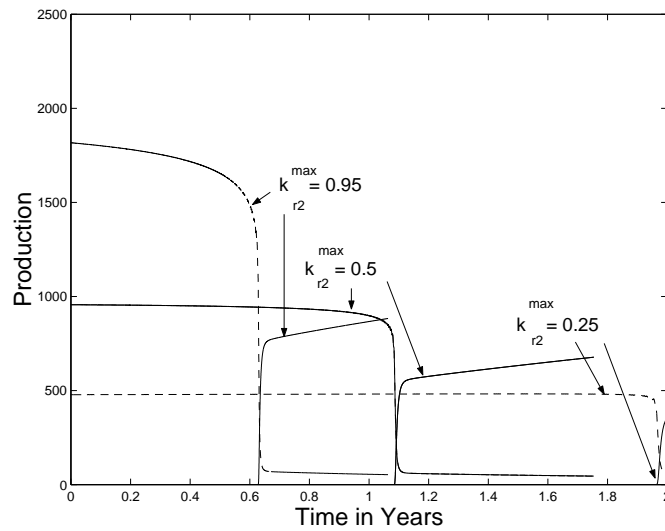


Figure 7: Production curves in barrels per day for different values of the maximum oil relative permeability. All further data are taken from Table 1. The dashed and solid curves respectively correspond to oil and water production.

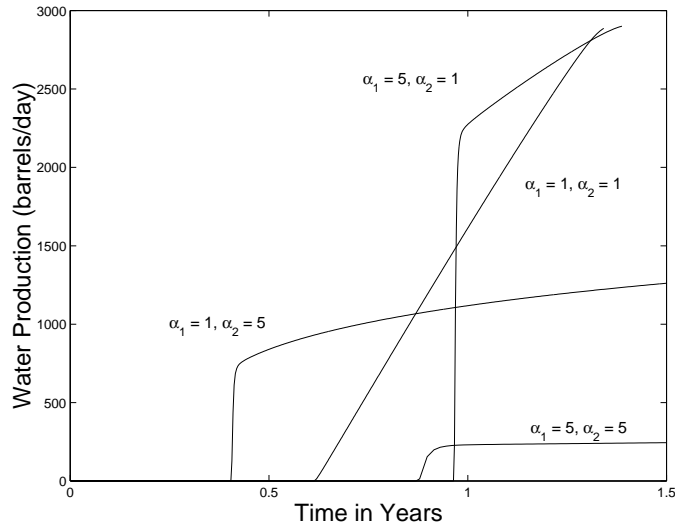


Figure 8: Production curves of water for different values of the exponents in the power-law relative permeability functions. All further data are taken from Table 1.

Remarks

Effects of the connate water and residual oil saturation can be analysed with a simple dimensional transformation. Hence this is omitted in this study.

The water relative permeability can have very curved shapes for low sorting factors. For high sorting factors the behaviour of the water relative permeability converges towards a third power. The shape of the oil relative permeability is less sensitive to changes of the sorting factor. Therefore, in next Section we abandon the Corey-permeability function and we use the power-law relative permeability functions.

4.2.2 Power-law relative permeability functions

In this section we investigate the influence of the shape of the relative permeability functions on the production of water and oil. For reasons stated before we only vary the exponents α_1 and α_2 . For $\alpha_i < 1$ the shape of the relative permeability function is concave and for $\alpha_i \geq 1$ the curve is convex.

For $\alpha_1, \alpha_2 > 1$ the fluxfunction $f(S_1)$ is convex-concave. We consider only non-concave relative permeabilities, i.e. $\alpha_i \geq 1$.

Figure 8 shows the water production as a function of time. It can be seen that water breakthrough takes place at a later time-step for α_1 large (convex water relative permeability function) and α_2 equal to one. However, after this breakthrough the water production is very large. Further, the case that both the water and oil relative permeability functions are convex ($\alpha_1 = \alpha_2 = 5$) also gives a late breakthrough (slightly earlier than the former case). After the breakthrough the water production is not so large. The case that both permeabilities are linear (viz. the test-case) gives a rather early breakthrough. The case that $\alpha_1 = 1$ and $\alpha_2 = 5$ gives very early water breakthrough. This case is least favourable.

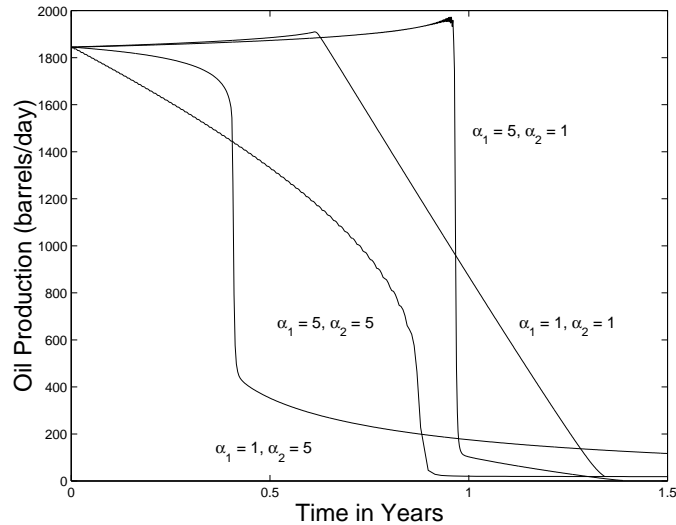


Figure 9: Production curves of oil for different values of the exponents in the relative permeability functions. All further data are taken from Table 1.

Figure 9 shows the oil production as a function of time for the same input-data as in Figure 8. It can be seen that the oil production remains a high level for a long time for the case that $\alpha_1 = 5$ and $\alpha_2 = 1$. Least advantageous is again the case that $\alpha_1 = 1$ and $\alpha_2 = 5$.

From this it follows that a convex shape of the water relative permeability function and a linear oil relative permeability is most favourable.

5 Conclusions

We have presented an accurate numerical method to predict oil and water recovery for cylindrical flow towards a well in the center. The flow problem is considered representative for injection well treatment with polymer gels. We investigated the influence of the shape of relative permeability functions. After comparison of the production behaviour we conclude the following:

1. A low sorting factor for the water relative permeability (a high power law exponent) leads to considerable delay of water production without affecting the oil production rate. Such a low sorting factor would be the most desirable effect of permeability modifiers. However, in case of gravity segregation the positive effect vanishes.
2. A low water end-point permeability causes a reduction of the oil production rate. However, we also observe a delayed water production. A high oil end-point permeability is conducive to higher production rates.
3. Linear relative permeability for oil are conducive to better production rates.

Acknowledgements

We acknowledge the two-dimensional calculations done by drs. Matthijs de Rooij which gave us a better understanding. This work was funded by the European Union (Welgel project) and by the Welgel industrial consortium (BGplc, GDF, Halliburton, Norsk Conoco, Petrobras, Shell, SNF-Floerger, Statoil, Tarim Oilfield, Texaco and Total).

References

- [1] M.R. Avery, L.A. Burkholder, and M.A. Gruenenfelder. Use of crosslinked xanthan gels in actual profile modification field projects. *Society of Petroleum Engineers (SPE)*, paper 14114, presented in Beijing March 1986, 1986.
- [2] R.H. Brooks and A.T. Corey. Properties of porous media affecting fluid flow. *J. Irrig. and Drain. Div. (Proc ASCE) IR 2*, 92:61–88, 1966.
- [3] M. de Rooij. *Impact of polymer gels on flow in the near well region*. TA/PW 99.003. Delft University of Technology, Delft, December 1999. Master’s Thesis.
- [4] S.S. Nagra, J.P. Batycky, R.E. Nieman, and J.B. Bodeux. Stability of waterflood diverting agents at elevated temperatures in reservoir brines. *Society of Petroleum Engineers (SPE)*, paper 15548, 1986.
- [5] G.J.M. Pieters. *De invloed van relatieve permeabiliteitsfuncties in een olie reservoir op de olie- en water productie*. Delft University of Technology, Delft, December 1999. Intermediate report, in Dutch.
- [6] H.K. Rhee, R. Aris, and N.R. Amundson. *First-order partial differential equations, Theory and application of hyperbolic systems of quasi-linear equations*. Prentance-Hall, Englewood Cliffs, 1969.
- [7] J. Smoller. *Shock waves and reaction-diffusion equations*. 1. Springer, New York, 1983.
- [8] B. van Leer. Towards the ultimate conservative difference scheme. iii. upstream-centered finite-difference schemes for ideal compressible flow. *Journal of Computational Physics*, 23:276–299, 1977.

Appendix 1: Linear Test-case

We consider a test-case in which we have linear relative permeabilities, let them be given by:

$$k_{r1} = S_1,$$

$$k_{r2} = 1 - S_1.$$

Substitution of above relation into the flux-function (see equation 2.6) gives:

$$f(S_1) = \frac{1}{1 + \frac{\mu_1(1-S_1)}{\mu_2 S_1}} =: \frac{1}{1 + E \frac{1-S_1}{S_1}}, \quad (5.1)$$

which we use for solving

$$\frac{\partial S_1}{\partial t} + Q(t) \frac{\partial f(S_1)}{\partial x} = 0. \quad (5.2)$$

Since $\mu_1 < \mu_2$ we have $E < 1$ and $f(S_1)$ is therefore a concave function. From the initial and boundary condition follows that shocks are not stable and rarefactions occur, i.e. $S_1(x, t)$ is continuous in x for $t > 0$ (see e.g. Smoller [7], Rhee et al [6]). We look for self-similar solutions that satisfy

$$S_1(x, t) = \bar{S}_1(\eta), \quad \eta := \frac{x}{\int_0^t Q(s) ds}. \quad (5.3)$$

Substitution of (5.3) into (5.2) gives

$$\bar{S}'_1(\eta) = 0 \text{ or } f'(\bar{S}_1) = \eta. \quad (5.4)$$

The first solution corresponds to a constant state, the second to a state in which \bar{S}_1 depends on η . From the derivative of $f(S_1)$, equation (5.4) can be arranged into

$$\bar{S}_1(\eta) = \frac{\sqrt{\frac{E}{\eta}} - E}{1 - E}.$$

Note that S_1 must be a decreasing function in order to be continuous. The overall solution in x and t can be written as (for all $0 < t < \tau_1$):

$$S_1(x, t) = \begin{cases} 1, & 0 \leq x \leq \eta_L \int_0^t Q(s) ds, \\ \frac{\sqrt{\frac{E \int_0^t Q(s) ds}{x}} - E}{1 - E}, & \eta_L \int_0^t Q(s) ds < x < \eta_R \int_0^t Q(s) ds, \\ 0, & \eta_R \int_0^t Q(s) ds \leq x \leq L. \end{cases}$$

We define τ_1 as the time at which $\eta_R \int_0^{\tau_1} Q(s) ds = L$ and $\tau_2 > \tau_1$ is defined as the time at which $\eta_L \int_0^{\tau_2} Q(s) ds = L$. The parameters (η_L, η_R) are determined from continuity, i.e.

$$\begin{cases} 1 = \bar{S}_1(\eta_L), \\ 0 = \bar{S}_1(\eta_R), \end{cases}$$

which gives

$$\eta_L = E < 1 \quad \text{and} \quad \eta_R = \frac{1}{E} > 1.$$

The velocity $Q(t)$ is determined from equation (3.5):

$$Q(t) = - \frac{k_0 \Delta p}{\int_0^L \frac{dx}{(R^2 - 2x) \left(\frac{S_1}{\mu_1} + \frac{1 - S_1}{\mu_2} \right)}} =: - \frac{k_0 \Delta p}{I}. \quad (5.5)$$

The integral in above equation can be decomposed into three parts for $t < \bar{\pi}$:

$$I = \mu_1 \int_0^{x_L(t)} \frac{dx}{R^2 - 2x} + \sqrt{\frac{\mu_1 \mu_2}{\int_0^t Q(s) ds}} \int_{x_L(t)}^{x_R(t)} \frac{\sqrt{x}}{R^2 - 2x} dx + \mu_2 \int_{x_R(t)}^L \frac{dx}{R^2 - 2x}.$$

Here $x_L(t) := E \int_0^t Q(s) ds$ and $x_R(t) := \frac{1}{E} \int_0^t Q(s) ds$. In this appendix we only consider times $t < \tau_1$, it is obvious that the integral (5.5) can be decomposed into two parts for $\bar{\pi} < t < \tau_2$ and one part for $t > \tau_2$. Calculation of these integrals is straightforward, for completeness we give the result for the second part:

$$\int \frac{\sqrt{x}}{R^2 - 2x} dx = \frac{R}{\sqrt{2}} \left\{ \operatorname{arctanh} \left(\sqrt{\frac{2x}{R^2}} \right) - \sqrt{\frac{2x}{R^2}} \right\},$$

with $\operatorname{arctanh}(x) := \int_0^x \frac{dt}{1-t^2}$. Hence the integral I , with $\xi(t) := \int_0^t Q(s)ds$, becomes

$$I = \frac{\mu_1}{2} \ln \left(\frac{R^2 - 2E\xi(t)}{R^2} \right) + \frac{\mu_2}{2} \ln \left(\frac{R^2 - 2L}{R^2 - \frac{2\xi(t)}{E}} \right) + \frac{1}{E} \sqrt{\frac{\mu_1\mu_2}{2\xi(t)}} \left\{ \operatorname{arctanh} \left(\sqrt{\frac{2\xi(t)}{ER^2}} \right) - \sqrt{\frac{2\xi(t)}{ER^2}} - \operatorname{arctanh} \left(\sqrt{\frac{2E\xi(t)}{R^2}} \right) + \sqrt{\frac{2E\xi(t)}{R^2}} \right\} =: I(\xi(t)).$$

Substitution of above integral into equation (5.5) gives an ordinary differential equation (ODE) in $\xi(t)$:

$$Q(t) = \xi'(t) = \frac{k_0 \Delta p}{I(\xi(t))}.$$

Above ODE can be solved using standard methods to give an explicit solution for $\xi(t)$. After some tedious algebra, we obtain the following equation for $\xi(t)$:

$$\begin{aligned} & -\frac{\mu_1}{4E} [(R^2 - 2E\xi)(\ln(R^2 - 2E\xi) - 1) - R^2(\ln(R^2) - 1)] + \\ & \quad + \xi \left[\frac{\mu_2}{2} \ln(R^2 - 2L) - \frac{\mu_1}{2} \ln(R^2) \right] + \\ & \quad + \frac{E\mu_2}{4} \left[\left(R^2 - \frac{2\xi}{E} \right) \left(\ln \left(R^2 - \frac{2\xi}{E} \right) - 1 \right) - R^2(\ln(R^2) - 1) \right] + \\ & \quad + \sqrt{\frac{\mu_1\mu_2}{2R^2}} \left(\sqrt{\frac{2}{R^2}} \left(\sqrt{E} - \sqrt{\frac{1}{E}} \right) \xi + \right. \\ & \quad \left. + \frac{ER^2}{2} \left\{ 2\sqrt{\frac{2\xi}{ER^2}} \operatorname{arctanh} \left(\sqrt{\frac{2\xi}{R^2E}} \right) + \ln \left(1 - \frac{2\xi}{ER^2} \right) \right\} - \right. \\ & \quad \left. - \frac{R^2}{2E} \left\{ 2\sqrt{\frac{2E\xi}{R^2}} \operatorname{arctanh} \left(\sqrt{\frac{2E\xi}{R^2}} \right) + \ln \left(1 - \frac{2E\xi}{R^2} \right) \right\} \right) = -k_0 \Delta p \cdot t. \end{aligned}$$

We are not able to find an explicit solution for above equation. Above equation is solved numerically using a zero-point method. Above equation is advantageous with respect to time integration of the ODE:

- there are no problems concerning stability,
- at any time the solution can be obtained quickly without doing the whole time-integration.

Finally we remark that it is a trivial exercise to extend above solution to the case of a more general linear relative permeability function. Since this does not contribute to clarity, it is omitted here.